Monitoring of solids behaviour during gravitional flow in rectangular silo

M. Niedostatkiewicz [1], Z. Chaniecki [2], K.Grudzień [2], A. Romanowski [2], R.Banasiak [2], J.Betiuk [2]

[1] *Department of Fundamentals of Building and Material Engineering, Technical University of Gdańsk*
mniedost@pg.gda.pl

[2] *Computer Engineering Department, Technical University of Łódź*
zch@kis.p.lodz.pl

Reviewer: H. Wang (Tianjin University, China)

Summary: This paper is focused on the application of Electrical Capacitance Tomography (ECT) to gravitational flow of bulk solid in rectangular silo investigation. In order to measure the materials distribution inside a vessel, a dedicated, spatial 16 electrode sensor is designed. Reconstructed images are presented in 3D domain space. The investigated silo model consists of rectangular bin and a cone-like hopper section. The flow behaviour of material (friable sand) is studied for two silo model configurations having different lower section slopes. The slope angle is a silo geometrical parameter affecting the type of the flow regime - mass or funnel type.

Keywords: ECT, bulk solid concentration measurement, rectangular silo investigation, processes monitoring, 3D imaging

1. Introduction

The behaviour of granular materials during confined silo flow is very complex among others due to appearance of localization of deformation in the form of narrow zones of intense shearing (Tejchman et al., 2000). The shear zones occur along silo walls, as well, as inside flowing (initially dense) granular material for both: bin section (Fig. 1) with rough walls and hopper section no matter of the wall roughness (Tejchman 1997). The presence of wall shear zones significantly influences stresses along the walls. In turn, the appearance of shear zones inside of the flowing material causes significant quasi-static fluctuations of wall stresses and a flow asymmetry (Rechenmacher, 2006). The width of shear zones depends on many factors such as: initial solid density, mean grain diameter of solid, wall roughness, specimen size, pressure level, direction of deformation and flow velocity (Tejchman et al., 2000; Yoshida et al., 1994; Nübel, 2002). The knowledge of the deformation field in the silo fill is very important in order to explain the mechanism of the granular flow behaviour in silos.

At present, the Particle Image Velocimetry (PIV) is one of the non-invasive methods to quantify local displacements in solids. This technique is used for measuring surface displacements on the basis of the numerical analysis of digital photographs successive pairs. Photographs pairs of the side of deformed specimen are taken with a CCD-camera (charge couple device). PIV method was also used for observation of bulk solid behaviour in rectangular model silo. Shear zones, along the silo vertical walls and inside the flowing material were detected on the basis of deviatoric and volume strains (Niedostatkiewicz and Tejchman, 2005; Slominski et al., 2006, 2007).

The main aim of this paper is to present the preliminary results of the 3D concentration distribution of bulk solid during rectangular silo discharging (Wajman et al., 2007; Romanowski et al., 2006, 2007; Chaniecki et al., 2006). The prepared measurement computer system based on ECT unit makes it easier to investigate the physical phenomena which take place in the rectangular silo. The description of the shear zone is very important. The concentration measurement of solid (porous) is crucial to control the silo loading and emptying for both, model (laboratory) scale, as well, as for industrial application. The knowledge of the porous spatial distribution is decisive for the determining of the real distribution of solid pressure in silo. The accurate analysis of the spatial distribution may allow to diagnose the adverse phenomena, especially the dynamics effects, which take place during silo discharging. The understanding of dynamic effects enables to eliminate or minimize their dangerous occurrence.

The conducted experiments concerned the investigation of influence the following considerations on material behaviour during silo discharging process.:

- the regime flow (mass flow or funnel flow);
- the initially packing slid density;
- the wall roughness;

The presented results concern the case of mass flow with initially dense sand. Two types of wall roughness are analysed; smooth and rough wall silos.

2. Experimental setup

The model tests were carried out with two rectangular perspex symmetric model silos (mass flow silo and funnel flow silo) consisting of a bin and a hopper (Fig. 1). The same models were used both for PIV and ECT tests. The height of a mass flow silo was h=0.32 m, the width b=0.09 m, the depth d=0.07 m. In turn, the height of a funnel flow silo was h=0.29 m, the width b=0.15 m, the depth d=0.07 m. The width of the rectangular outlet along the silo depth in both models was 5 mm. The wall thickness was 0.01 m.

The tests were performed with a dry, cohesionless sand with a mean grain diameter d50=1.0 mm and uniformity coefficient U=5. An initially dense sand (γ=16.5 kN/m3, e0=0.61) was obtained by filling the silo using a so-called “rain method” (through a vertically movable sieve located always 25 mm above the upper sand surface in the symmetry-axis). In turn, an initially loose sand (γ=15.5 kN/m^3, e_0 =0.70) was

obtained by filling the model silo from a small feeder hopper fixed above the silo. The silos were emptied gravitationally; the mean outflow velocity was approximately v=10 mm/s. The total emptying time of the mass flow silos was about 30 s. Smooth and very rough walls in a bin and a hopper were used. A wall surface with a high roughness was obtained by gluing a sand paper to the interior wall surfaces (rw≈d50). All experiments were performed in an air-conditioned room with constant temperature of 20 °C and relative humidity of 50%.

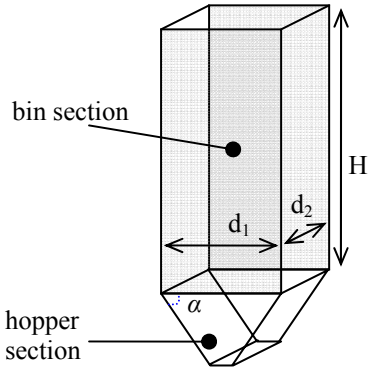

Fig. 1. Silo model with bin and hopper sections indicated.

3. Particle Image Velocimetry tests

The results of concentration distribution inside silo obtained with aid of ECT system are compared to the results acquired using PIV methodology (Slominski et al., 2006, 2007). Special emphasis was placed on region close to the silo wall. Until now, this region could be investigated only with CCD camera or image processing using PIV. This kind of analysis allows to compare only the regions next to Perspex silo wall.

3.1. Methodology of PIV measurement

The PIV system interprets differences in light intensity as a gray-scale pattern recorded at each pixel on CCD camera. For each point in the image plane, a scalar value which reflects the light intensity of the corresponding point in the physical space is assigned. Hence, PIV maps simply the light energy of and individual particle in a physical space into an intensity value in the image plane - greyscale pattern. The gray levels range from 0 (“real black”) to 255 (“pure white”) for an 8-bit image.

The whole procedure can be summarized as follows (Nübel, 2002; White et al., 2003; Hutter and Kuerchner, 2003):

1. subdivide the image into interrogation cells:
2. calculate the image intensity fields at time t and t+Δt for one interrogation cell:
3. calculate the correlation between image intensity fields (most likely displacement is the peak of the function);
4. repeat the procedure for each interrogation cell,
5. convert the Eulerian deformation field into Lagrangian deformation field,
6. calculate strain tensor εv.

3.2. PIV experimental results

The results for the smooth walls silo show the distribution of the volumetric and deviatoric strains are non-uniform (Fig. 2). The strains were significantly larger for initially dense sand (3-5 times) comparing to initially loosely packed sand. The minimum volumetric strain (contractancy) and maximum volumetric strain (dilatancy) were about 0.06% and 0.09% (loose sand) and 0.28% and 0.3% (dense sand), respectively (for t=7s, Fig.2a). The deviatoric strain changed between 0%-0.09% (loose sand) and 0%-0.5% (dense sand) (Fig. 2b). Densification zones were mixed with loosening ones. In the case of initially dense sand, several curvilinear dilatant zones occurred in the hopper and one pronounced parabolic in the bin. The dilatant zones were created in the neighborhood of the outlet. The material was sheared not only inside of the material, but also along the walls. The width of the wall shear zone was 7 mm (initially dense sand, smooth walls). The distribution of the volumetric and deviatoric strain in a model silo with very rough walls is less non-uniform (Fig. 3) than in a silo with smooth walls. The strains increase with decreasing initial density. The minimum volumetric strain (contractancy) and maximum volumetric strain (dilatancy) were about 0.015% and 0.04% (loose sand), 0.08% and 0.2% (medium dense sand) and 0.1% and 0.4% (dense sand), respectively (at t=7 s, Fig. 3a). The deviatoric strain changed between 0%-0.06% (loose sand), 0%-0.2% (medium dense sand) and 0%-0.3% (dense sand), respectively (Fig. 3b). The dilatant and contractant zones appeared in the entire silo. The shape of dilatant zones was chaotic in initially loose and medium dense sand. In initially dense sand, their shape was more regular (parabolic) in the bin (Fig. 3). The material was subject to shearing at walls and inside of the fill mainly in initially dense sand. The width of the wall shear zone was 12 mm (initially dense sand, very rough walls).

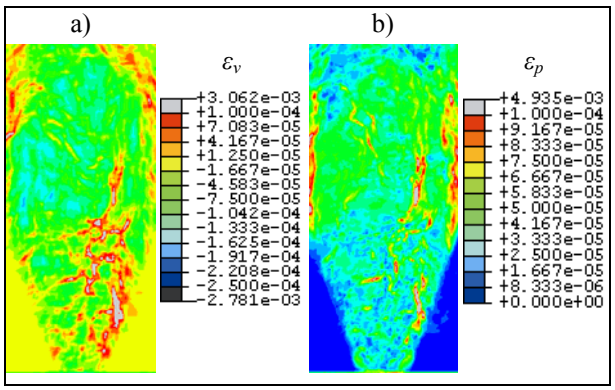

Fig.2: Evolution of the volume strain ε_v (a) and deviatoric strain ε_p (b) in a mass flow silo after 7 s of flow for the smooth wall silo

4. Electrical Capacitance Tomography tests

As opposed to PIV methods electrical capacitance tomography allows to investigate not only the silo area at wall but also inner space. The role of applied ECT system, based on charge/discharge measurement procedure (Williams and Beck, 1995; Pląskowski et al., 1995), in the first investigation stage was measuring the concentration in areas corresponding to these studied with PIV methods – close to the silo walls.

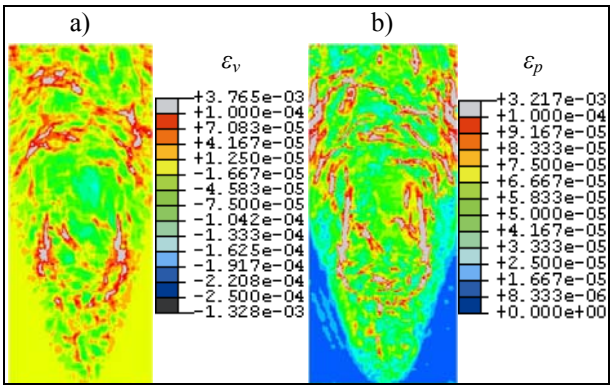

Fig.3: Evolution of the volume strain ε_v (a) and deviatoric strain ε_p (b) in a mass flow silo after 7 s of flow for the rough wall silo

4.1. Methodology of ECT measurement

In order to investigate the bulk solid behaviour in rectangular silo, a dedicated set of the planar sensors was developed. The used tomography system allows to connect maximum 32 electrodes. During the conducted measurements the number of electrodes was 16. In the future it seems to be necessary to extend the electrodes number to 32 (Fig. 4).

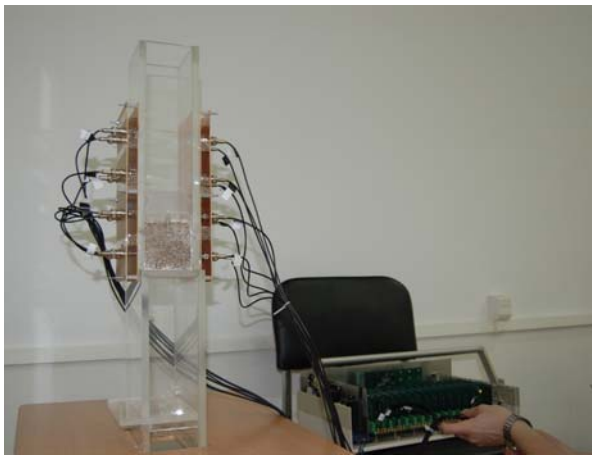

Fig.4 Laboratory silo model and ECT system photo.

Two vertical planes of electrodes were located on opposite silo walls. Each plane of sensors consisted of 8 rectangular electrodes. However, the measurements were taken not only between pair of electrodes at the same sensor plane but also between the electrodes at different planes. Therefore, the measurement records set includes 120 capacitances.

4.2. 3D image reconstruction

Before conducting the measurements, corresponding sensitivity matrix ***S*** for applied sensor, was calculated (Yang and Peng, 2003; Lionheart, 2004). The sensitivity of each 3D elements (voxels) inside the sensor space defines the influence of the permittivity change inside this element on the change of the capacitance between the electrode pairs. The analysis of electrical field inside sensor space, based on 3D FEM modelling (Fig. 5a) – i.e. forward problem processing, allows to calculate the sensitivity map for each pair of electrodes. Slight simplification concerning the electrodes shape was assumed during numerical analysis. The electrodes were assumed to have the circular shape (Fig. 5b,5c).

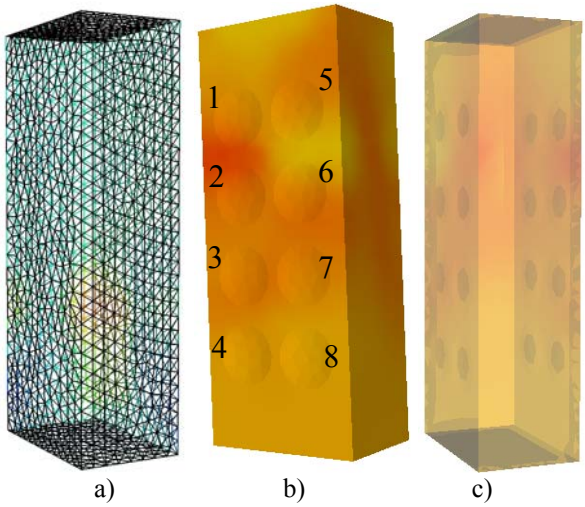

Fig. 5. Numerical model of the rectangular silo measurement space. a)FEM discretizing mesh b)electrodes numbering system, front view c)electrodes locations, side view.

The calculated sensitivity matrix allows to solve the inverse problem in ECT (Yang and Peng, 2003; Lionheart, 2004). In order to reconstruct the 3D tomography image, the most common algorithm, Linear Back-Projection (LBP), was applied (1):

$$\widetilde{\varepsilon}_{Mx1} = S^T_{MxN} \cdot C_{Nx1} \qquad (1)$$

where $\widetilde{\varepsilon}$ is the permittivity distribution column-vector (M=12422 - number of voxels), $C_t = \left[c_t^1, c_t^2, \ldots, c_t^N\right]^T$ is a measurements column-vector (N =120 - number of measurements).

Fig. 6 presents sensitivity maps for chosen electrode pairs for various spatial configurations of measurements.

4.3. ECT experimental results

In case of ECT results (comparing to PIV methodology) the concentration distribution can be visualized in several ways. However, the main feature of ECT measurements is enabling to look into the silo interior. The sandpaper was located inside silo, on the narrow walls. In order to investigate the influence of the silo wall roughness on the material flow behaviour, the reconstructed concentration distribution is presented in

form of the cuboidal images, where it is possible to observe the material concentration close to the silo wall.

Fig. 7 presents the changes of the mean normalized capacitance measurements in time (2):

$$\overline{C}_t = \sum_{i=1}^{N} c_t^i \qquad (2)$$

The data acquisition rate was at the level of 50 frames per second which gives the 20 millisecond time unit (frame) on the charts in the paper. There are also presented images corresponding to chosen time points from the plot to show the respective 3D representation of the material distribution.

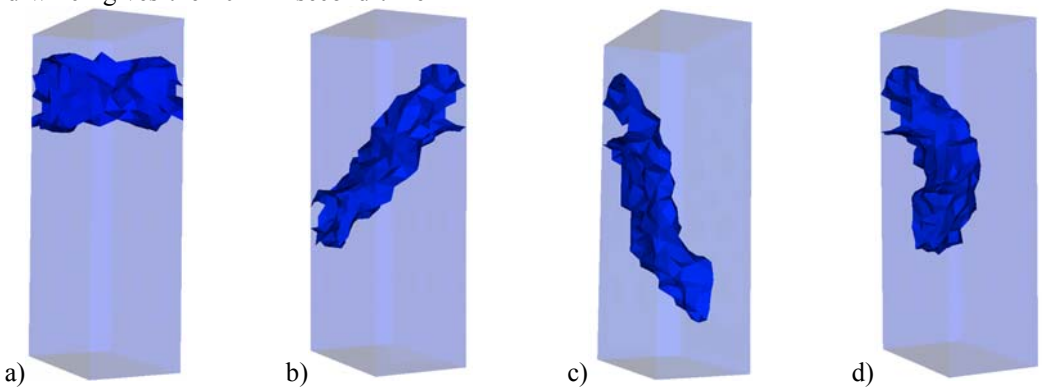

Fig. 6 Set of sensitivity maps for various electrode pairs configurations., a) s1-13, b) s1-15, c) s1-12, d) s1-7.

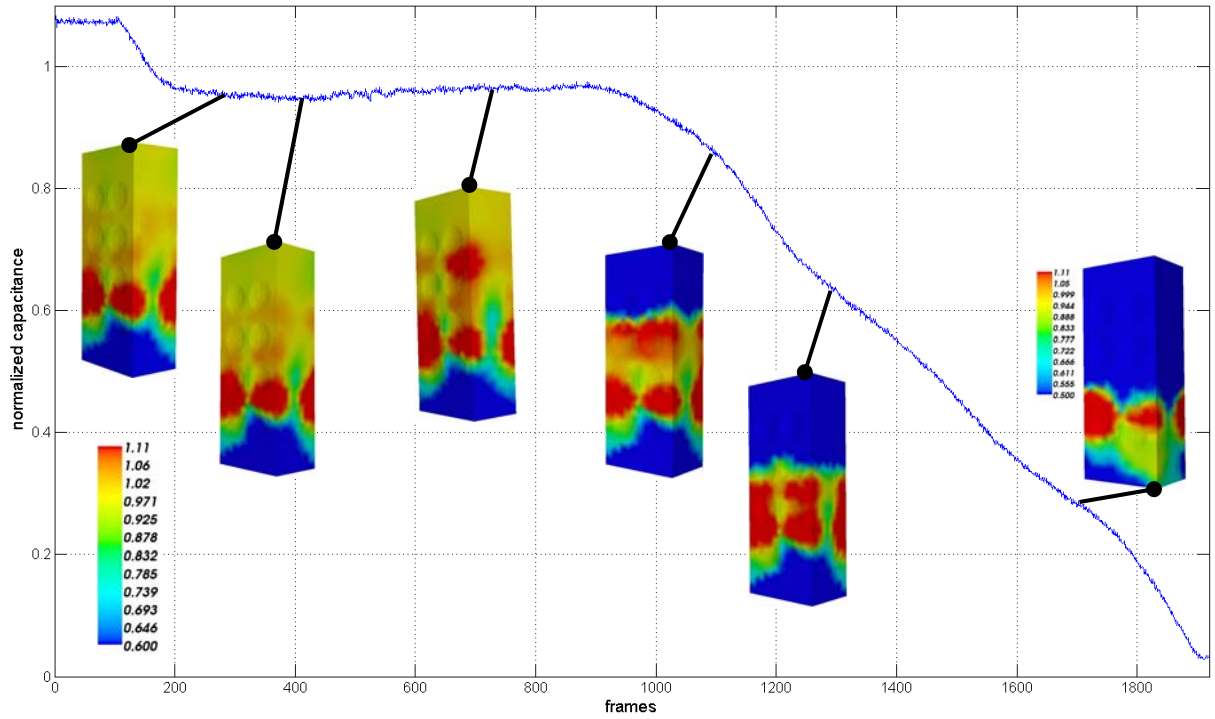

Fig. 7. Characteristic plot of the silo discharging process illustrated additionally with 3D images corresponding to several phases (distinct points indicated on the plot) of the process. The case for sandpaper with grit size 16 (extra course) stick to the silo wall.

The characteristic plot of the measurements capacitance changes is correct comparing to the theoretical expectations (Jenike, 1964). Since the silo is emptying, the capacitance records take lower values. It is possible to distinguish two, more significant changes of measurements. The first occurs just after opening the silo outlet (about 100 frame), the second (about 900 frame) when the flowing material surface appears at the highest part of sensor (electrodes number 1, 5 and 9, 13). The segment between the 100 and 900 frame is stabilized. In order to better illustrate the small changes of concentration, the scale of presented tomography

images is switched to <0.6, 1.1>, in contrast to the usual scale of the normalized tomography images <0, 1>. The blue colour represents the area with normalized concentration smaller than 0.6. This concentration value appears in higher parts of silo after 900 frame, which is obvious due to air appearing in the sensor space. The blue colour before 900 frame is related to the sensor located by the hopper section of silo. Fig. 8 presents the position of electrodes in the lower section. During experiment the area between the hopper section and the wall (the underline area – empty space) was filled by sand. The rest of the electrodes area (the active part of electrodes) located at lowest height is not sufficient to measure small changes of material concentration, which take place during silo discharging. This causes to generate the blue colour in lower part of silo images. Therefore, the region taken into consideration for analysis of the lower silo section should be carefully determined in order to perform relevant study.

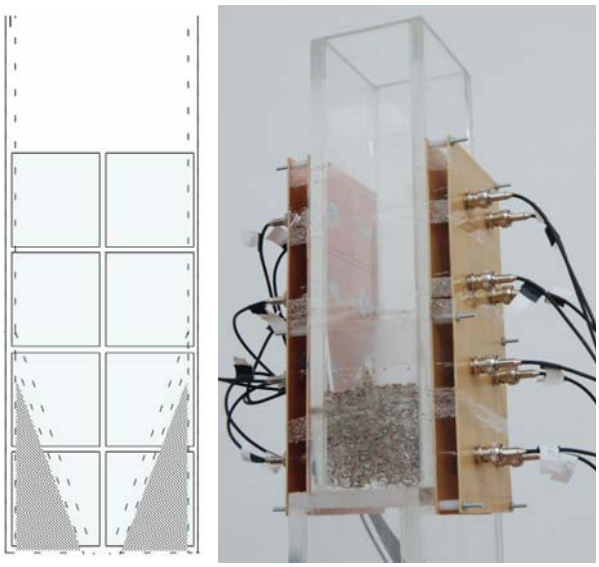

a) *b)*

Fig. 8 The sensor position relatively next to hopper section, a) scheme b) sensor position on the model

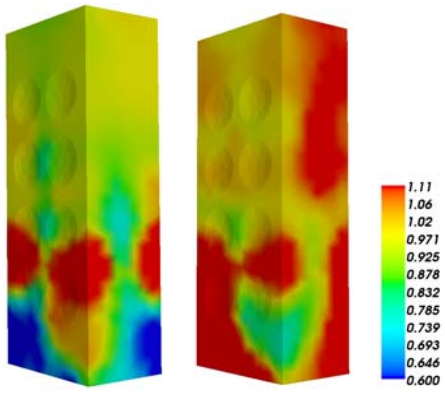

a) *b)* *c)*

Fig. 9 The concentration distribution in the stabilization part of the silo discharging process characteristic, a) roughness wall, b) smooth wall, c) scale.

For the purpose of comparison of the results obtained with PIV methodology, it is necessary to find the possibility of determining the shear zone. Fig. 9a presents example of 3D tomography image for a sandpaper (grit size 60 - medium), stuck to the interior wall. The last example (Fig. 9b) shows the 3D concentration distribution for the smooth silo wall. Comparison of the concentration distribution at the silo wall for three cases (smooth, medium and coarse sandpaper) reveals, that the shear zone is more visible for rough wall (with the sandpaper inside silo). The comparison of the shear zones for both cases with the rough walls seems not to be easy. At current stage of research, it can be concluded the shear zone is slightly more visible for sandpaper with grit size 16 (extra coarse).

5. Conclusions

On the basis of the PIV experimental results it can be concluded that those methods can be used as an effective optical technique to measure deformations on the surface of granular materials. However, PIV analysis require to be based on processing the successive digital images without any physical contact with process. Its main disadvantage is no possibility of tracing the strains inside the material; only these on the surface of the given specimen are possible to analyse. In the case of silo flow, due to wall friction between the granulate and transparent wall, strains on the surface can differ from these inside of the material. Thus PIV technique is not a perfect tool of investigation for described type of container flows.

The experiments for granular silo flow with smooth and rough walls showed the distribution of the volumetric and deviatoric strain in the flowing sand is strongly non-uniform due to occurrence of dilatant and contractant zones. The distribution of the volumetric and deviatoric strain in a mass flow silo is less asymmetric and non-uniform for dense packed sand and for rough walls. In a mass flow silo with dense sand and rough walls, the dilatant zones become more regular. The thickness of the wall shear zone increases with increasing wall roughness and decreasing initial density.

The preliminary experiments, conducted with aid of the ECT system, show the possibility of application of this kind of measurement technique. Unfortunately, achieved quality of reconstructed images is not sufficient to perform the thorough analysis. However the current results allow to draw a conclusion, that based on ECT measurements, the concentration distribution depends on the wall roughness in a silo mass flow. The presented results, in case of ECT measurements, concern only dense packed sand and the conclusion are alike as for PIV methodology. The shear zone is visible for the rough silo wall. The main ECT advantage over PIV methodology is based on possibility of visualization of the whole silo interior. To develop the ECT based methodology, it is necessary to solve several problems. In order to improve quality of tomography images it is necessary to increase the electrode number, and hence the measurement records

number. In the future work the measurement number should be 496 (for 32 electrodes). The other direction for the measurement improvement is the reduction of the wall thickness by half of its present value. This should improve the quality of capacitance measurements, since the smaller change of the material concentration inside silo could then be detected during measurements.

Acknowledgements

The authors thank the Polish Ministry of Science and Higher Education for their support of this work (no. 167/6, PR UE/2007/7).

REFERENCE

CHANIECKI Z., DYAKOWSKI T., NIEDOSTATKIEWICZ M., SANKOWSKI D. (2006), Application of electrical capacitance tomography for bulk solids flow analysis in silos. *Particle and Particle Systems Characterization*, Vol. 23, pp 306-312.

HUTTER K., KUERCHNER N., (2003), PIV for Granular Avalanches, Dynamical Response of Granular and Powder Materials in Large and Catastrophic Deformations, *Springer-Verlag*, Berlin.

JENIKE AW., (1964), Storage and flow of solids, Bull. No. 123, Utah Engineering Experiment Station, University of Utah, Salt Lake City.

LIONHEART W.R.B., (2004), Review: Developments in EIT reconstruction algorithms: pitfalls, challenges and recent developments, *Physiological Measurement*, Vol. 25, pp. 125-142.

NIEDOSTATKIEWICZ M., TEJCHMAN J., (2005), Application of a Particle Image Velocimetry technique for deformation measurements of bulk solids during silo flow. *Powder Handling & Processing*, Vol. 17, pp. 216-220.

NÜBEL K., (2002), Experimental and numerical investigation of shear localization in granular materials, *Publication Series of the Institute of Soil and Rock Mechanics*, University of Karlsruhe, p. 62.

PLĄSKOWSKI A., BECK M.S., THORN R., DYAKOWSKI T., (1995), *Imaging Industrial Flows: Applications of Electrical Process Tomography*, IOP Publishing, Bristol, p. 232.

RECHENMACHER A.L., (2006), Grain-scale processes governing shear band initiation and evolution in sands. *Journal of the Mechanics and Physics of Solids* Vol. 54, pp. 22-45.

ROMANOWSKI A., GRUDZIEŃ K., BANASIAK R., SANKOWSKI D., (2007), Hopper Flow Measurement Data Visualization: Developments Towards 3D, 5th World Congress on Industrial Process Tomography, Bergen 2007, pp. 986-993.

ROMANOWSKI A., GRUDZIEN K., WILLIAMS R.A., (2006), Analysis and Interpretation of Hopper Flow Behaviour Using Electrical Capacitance Tomography, *Particle & Particle Systems Characterization*, Vol. 23, p. 297-305.

SLOMINSKI C., NIEDOSTATKIEWICZ M., TEJCHMAN J., (2006), Deformation measurements in granular bodies using a Particie Image Velocimetry technique. *Archives of Hydro-and Environmental Engineering*, Vol. 53, pp. 71-94.

SLOMINSKI C., NIEDOSTATKIEWICZ M., TEJCHMAN J., (2007): Application of particle image velocimetry (PIV) for deformation measurement during granular silo flow, *Powder Technology*, Vol. 173, pp. 1-18.

TEJCHMAN J., (1997), Modelling of shear localization and autogeneous dynamic effects in granular bodies. *Habilitation Monography*, University of Karlsruhe, 140, pp. 1-353.

TEJCHMAN J., GUDEHUS G., (2000), Verspannung, Scherfugenbildung und Selbsterregung bei der Siloentleerung. In Silobauwerke und ihre spezifischen Beanspruchungen (eds.: J. Eibl and G. Gudehus), Deutsche Forschungsgemeinschaft, Wiley-VCH, pp. 245 - 284.

WAJMAN R., BANASIAK R., MAZURKIEWICZ Ł., SANKOWSKI D., (2007), Reply to comments on Spatial imaging with 3D capacitance measurements, *Measurement Science and Technology*, vol. 18, pp. 3668-3670.

WHITE D.J., TAKE W.A., BOLTON M.D., (2003), Soil deformation measurements using particle image velocimetry (PIV) and photogrammetry, *Geotechnique*, Vol. 53, pp. 619-631.

WILLIAMS R.A., BECK M. S., EDS., (1995), *Process Tomography — Principles, Techniques and Applications*, Butterworth-Heinemann, Oxford, p. 507.

YANG WQ., PENG L., (2003), Image reconstruction algorithms for electrical capacitance tomography, *Measurement Science and Technology*, Vol. 14, r1-r14.

YOSHIDA T., TATSUOKA F., SIDDIQUE M., (1994), Shear banding in sands observed in plane strain compression, *Localisation and Bifurcation Theory for Soils and Rocks* (eds.: R. Chambon, J. Desrues and I. Vardoulakis), Balkema, Rotterdam, pp. 165-181.